Post-Translational Cleavage of HMW-GS *Dy10* allele improves the cookie-making quality in common wheat (*Triticum aestivum*)

Yan Wang
State Key Laboratory of Crop Gene Exploration and Utilization in Southwest China
Qing Chen
Triticeae Research Institute, Sichuan Agricultural University
Yang Li
Triticeae Research Institute, Sichuan Agricultural University
Zhenru Guo
Triticeae Research Institute, Sichuan Agricultural University
Caihong Liu
Triticeae Research Institute, Sichuan Agricultural University
Yongfang Wan
Rothamsted Research
Malcolm Hawkesford
Rothamsted Research
Jing Zhu
Triticeae Research Institute, Sichuan Agricultural University
Wang Wu
Triticeae Research Institute, Sichuan Agricultural University
Meiqiao Wei
Triticeae Research Institute, Sichuan Agricultural University
Kan Zhao
Triticeae Research Institute, Sichuan Agricultural University
Yunfeng Jiang
Triticeae Research Institute, Sichuan Agricultural University
Yazhou Zhang
Triticeae Research Institute, Sichuan Agricultural University
Qiang Xu
Triticeae Research Institute, Sichuan Agricultural University
Li Kong
Triticeae Research Institute, Sichuan Agricultural University
Zhien Pu

Triticeae Research Institute, Sichuan Agricultural University
Mei Deng
Triticeae Research Institute, Sichuan Agricultural University
Qiantao Jiang
Triticeae Research Institute, Sichuan Agricultural University
Xiujin Lan
Triticeae Research Institute, Sichuan Agricultural University
Jirui Wang
State Key Laboratory of Crop Gene Exploration and Utilization in Southwest China
Guoyue Chen
State Key Laboratory of Crop Gene Exploration and Utilization in Southwest China
Jian Ma
State Key Laboratory of Crop Gene Exploration and Utilization in Southwest China
Youliang Zheng
State Key Laboratory of Crop Gene Exploration and Utilization in Southwest China
Yuming Wei
State Key Laboratory of Crop Gene Exploration and Utilization in Southwest China
Pengfei Qi (pengfeiqi@hotmail.com)
Triticeae Research Institute, Sichuan Agricultural University https://orcid.org/0000-0002-7772-9591

Research Article

Keywords: HMW-GS, amino acid substitution, polymer size, wheat processing quality

Posted Date: March 16th, 2021

DOI: https://doi.org/10.21203/rs.3.rs-283101/v1

Version of Record: A version of this preprint was published at Molecular Breeding on August 17th, 2021. See the published version at https://doi.org/10.1007/s11032-021-01238-9.

Abstract

Wheat is a major staple food crop worldwide because of the unique properties of wheat flour. High molecular weight glutenin subunits (HMW-GSs), which are among the most critical determinants of wheat flour quality, are responsible for the formation of glutenin polymeric structures via interchain disulfide bonds. We herein describe the identification of a new HMW-GS *Dy10* allele (*Dy10-m619SN*). The amino acid substitution (serine-to-asparagine) encoded in this allele resulted in a partial post-translational cleavage that produced two new peptides. These new peptides disrupted the interactions among gluten proteins because of the associated changes to the number of available cysteine residues for interchain disulfide bonds. Consequently, *Dy10-m619SN* expression decreased the size of glutenin polymers and weakened glutens, which resulted in wheat dough with improved cookie-making quality, without changes to the glutenin-to-gliadin ratio. In this study, we clarified the post-translational processing of HMW-GSs and revealed a new genetic resource useful for wheat breeding.

Introduction

Common wheat (*Triticum aestivum* L.; AABBDD; 2n = 6x = 42) is an unusual food crop suitable for the production of various foods because of its unique processing quality, which is related to the continuous protein network in its grains (Shewry and Halford 2002). The gluten proteins, which are crucial components of the protein network, are composed of gliadins and glutenins. The gliadins are single-chain polypeptides that may function as plasticizers responsible for dough extensibility (Barak et al. 2015; Qi et al. 2006). Glutenins are multi-chain polymeric proteins composed of low and high molecular weight glutenin subunits (LMW-GSs and HMW-GSs, respectively) (Shewry et al. 1999).

As a ‘backbone’ for interactions with other glutenin subunits and gliadins, HMW-GSs are among the most important determinants of end-use quality, with key effects on dough strength and elasticity (Shewry et al. 2003a; Wieser 2007). The HMW-GS genes, which lack introns (Anderson et al. 1989), have been localized to the *Glu-1* loci on the long arm of chromosomes 1A (*Glu-A1*), 1B (*Glu-B1*), and 1D (*Glu-D1*) (Payne et al. 1982; Shewry et al. 2003b). Each locus contains two tightly linked genes encoding a smaller y-type subunit and a larger x-type subunit (Shewry et al. 1992). Normally, only 3–5 HMW-GSs are produced in common wheat (Payne et al. 1981). The HMW-GSs have a common primary structure, with a long central repetitive domain surrounded by highly conserved N- and C-terminal non-repetitive domains (Halford et al. 1992). The N-terminal domain generally has three or five cysteine (Cys) residues, whereas the C-terminal domain usually has one Cys and the central repetitive domain either lacks a Cys residue or has only one (Shewry and Halford 2002). The sequence length, structure, and expression level of HMW-GSs are wheat quality determinants. Furthermore, the number and distribution of Cys residues are important features of HMW-GSs because disulfide bonds between these residues determine the polymeric structure and conformation of proteins, which affect the dough strength (Shewry et al. 1992, 2003a).

The *Glu-D1* locus is a major genetic factor influencing the dough strength and bread-making quality of wheat. Previous studies on the effects of *Glu-1* on the wheat end-use quality revealed that *Dx5* and *Dy10*

are the alleles that produce the best subunit combination (Barro et al. 2003; Lawrence et al. 1988; Shewry et al. 2003a). As expected, the Dy10 subunit is positively associated with wheat processing quality (Blechl et al. 2007; Laudencia-Chingcuanco 2012; León et al. 2009).

Storage proteins are initially synthesized on the rough endoplasmic reticulum, where the signal peptide is cleaved. Most storage proteins are subject to further processing, including post-translational modifications (Müntz 1998). The post-translational cleavage of precursor storage proteins, which has been detected in rice (Kumamaru et al. 2010; Wang et al. 2009), castor bean (Hara-Nishimura et al. 1991), soybean (Hara-Nishimura et al. 1995), and Arabidopsis (Gruis et al. 2004), is an essential part of storage protein maturation. However, there have been relatively few reports describing the post-translational cleavage of wheat seed storage proteins.

In this study, a new *Dy10* allele, *Dy10-m619SN*, was identified by screening an ethyl methanesulfonate (EMS)-induced mutant population of the common wheat cultivar ‘Shumai 482’. A further analysis revealed that *Dy10-m619SN* expression results in three peptides in wheat seeds because of a post-translational cleavage. Additionally, the effects of *Dy10-m619SN* on wheat processing quality as well as the underlying mechanism were investigated.

Materials And Methods

Plant materials and growth conditions

‘Shumai 482’ (wild type; WT) is a common wheat (*Triticum aestivum*) cultivar released by the Triticeae Research Institute, Sichuan Agricultural University. Its HMW-GS composition is Ax1, Bx7 + By9, and Dx5 + Dy10 (Xu et al. 2018). The mutant was isolated from ‘Shumai 482’ seeds treated with 0.8% EMS (Sigma-Aldrich, St. Louis, MO, USA). The mutant seeds from the M_2 to the M_5 generations were analyzed by sodium dodecyl sulfate polyacrylamide gel electrophoresis (SDS-PAGE) to verify the mutation.

To analyze wheat processing quality, the mutant was backcrossed with the WT (Fig. S1, part a). Fourteen BC_2F_4 (seven with the WT genotype and seven with the mutant genotype) and 14 BC_3F_4 (seven with the WT genotype and seven with the mutant genotype) homozygous lines were grown at the experimental farm of Sichuan Agricultural University (30°43'16"N, 103°52'15"E) during the 2017–2018 and 2019–2020 wheat growing seasons, respectively. Field trials were performed using a randomized block design. Each homozygous line was planted in a 2 m × 2 m area, with 20 cm between rows and 60 plants per row. A compound fertilizer [N:P:K (15:15:15)] was applied before sowing at a rate of 450 kg per hectare. Additionally, six BC_2F_4 homozygous lines (three with the WT genotype and three with the mutant genotype) were also grown (250 plants per line) in a greenhouse with a 16-h light (23°C)/8-h dark (18°C) cycle as previously described (Zhang et al. 2017).

Mature grains were sun-dried and stored at room temperature for 60 days before analyses. The agronomic performance after backcrossing was recorded. The harvested WT and mutant seeds for each line were analyzed by SDS-PAGE and acid polyacrylamide gel electrophoresis (A-PAGE) (Fig. S1b).

The mutant was used as the female parent and crossed with the common wheat cultivar 'Chinese Spring' (HMW-GS composition: Bx7 + By8 and Dx2 + Dy12). The F_1 generation was allowed to self-pollinate in the greenhouse. The HMW-GS composition was determined in the F_2 generation by SDS-PAGE.

SDS-PAGE, A-PAGE, and immunoblot analyses

Gliadins were extracted and separated by A-PAGE as previously described (Yan et al. 2003). Additionally, an SDS-PAGE analysis was completed using a published procedure (Qi et al. 2011). Specifically, the protein extraction buffer consisted of 62.5 mM Tris-HCl, pH 6.8, 10% (v/v) glycerol, 2% (w/v) SDS, 0.002% (w/v) bromophenol blue, and 1.5% (w/v) dithiothreitol (DTT). The seed storage proteins for the A-PAGE and SDS-PAGE were extracted from 10 mg ground seed powder. A urea SDS-PAGE analysis was performed under the same conditions, but urea was added to the solutions before the gel polymerized for a final concentration of 4 M urea (Wang et al. 2018).

Immature WT and mutant seeds collected at 5, 8, 11, 14, 17, 20, 24, and 28 days post-anthesis (dpa) were ground to a fine powder in liquid nitrogen, after which storage proteins were extracted from 10 mg powder as described above to assess the post-translational cleavage by SDS-PAGE.

The relative proportions of each HMW-GS in mature seeds were determined using 200 WT and mutant seeds. The seed storage proteins, including the HMW-GSs, were extracted from 10 mg powder per seed as described above. The extracted HMW-GSs were separated by SDS-PAGE. The proportions of HMW-GSs (Ax1, Bx7 + By9, and Dx5 + Dy10) were determined using the Quantity One software (Bio-Rad, Hercules, CA, USA) as previously described (Wan et al. 2014).

The extra protein in the mutant was confirmed as a HMW-GS with the rabbit anti-HMW-GS polyclonal antibody (1:4,000; Denery-Papini et al. 1996) and the HRP-conjugated anti-rabbit secondary antibody (1:8,000; Sigma-Aldrich). The extracted proteins were separated by SDS-PAGE and then electrophoretically transferred to a PVDF membrane (Invitrogen, Carlsbad, CA, USA). After washing twice with TBST [Tris-buffered saline with 0.05% (v/v) Tween-20], the membrane was blocked for 1 h with 1% bovine serum albumin in TBST. The membrane was incubated with the primary antibody for 2 h followed by the secondary antibody for 1 h. After washing three times with TBST, the immunoblot was visualized with the Pierce™ ECL Plus Western Blotting Substrate (Thermo Fisher Scientific, Waltham, USA).

Mass spectrometry and C-terminal sequencing

For the mass spectrometry analysis, the band corresponding to the extra protein in the mutant was excised manually from the SDS-PAGE gel. The protein was digested with trypsin, after which the resulting tryptic peptides were identified by mass spectrometry analysis, which was completed by Qitai Biotechnology (Nanjing, China).

Regarding the C-terminal sequencing, the targeted proteins from the WT and mutant samples were digested with chymotrypsin and identified by liquid chromatography–mass spectrometry analysis, which

was completed by Bio-Tech Pack Technology (Beijing, China).

DNA/RNA extraction, gene cloning, and sequencing

Genomic DNA was extracted from fresh leaves as previously described (Doyle and Doyle 1987). A pair of allele-specific PCR primers (F1/R1) (Table S4) were designed based on the published HMW-GS gene sequences. A high-fidelity La-Taq polymerase (Takara, Dalian, China) was used for cloning the complete coding sequence (CDS). The PCR products were separated on a 1.5% agarose gel, and the expected fragment was purified and inserted into the pMD19-T vector (Takara). Positive colonies were sequenced by Sangon Biotech (Shanghai, China). Both the cloning and sequencing experiments were repeated independently at least three times.

Immature WT and mutant seeds (25 dpa) were collected and ground to a fine powder in liquid nitrogen. Total RNA was extracted from the powder using the MiniBEST Universal RNA Extraction Kit with DNase (Takara). The RNA concentration was determined with the NanoDrop One Spectrophotometer (Thermo Fisher Scientific). The RNA samples were reverse transcribed using the Prime Script™ 1st Strand cDNA Synthesis Kit (Takara). The CDS and the 3' untranslated region (UTR) of the *Dy10* allele in the WT and mutant were cloned with primers F2/R2 (Table S4) and the cDNA.

Genotyping analysis by Kompetitive Allele-Specific PCR (KASP)

The genotypes were confirmed by KASP genotyping (LGC Genomics, Teddington, Middlesex, UK). Briefly, genomic DNA samples from the WT, mutant, and their hybrid progeny (F_1 generation) were diluted to a uniform concentration. The equivalent of 50 ng DNA per sample was used for genotyping. The KASP primers (F5/F6/R5 or R6) (Table S4) were designed according to the manufacturer's protocols. The experiment was completed with the Master Mix and the CFX96™ Real-Time PCR system (Bio-Rad).

Expression of *Dy10* alleles in *Escherichia coli*

The *Dy10-m619SN* gene sequence was re-amplified using the F3/R3 primer pair (Table S4) to remove the signal peptide sequence and to add *Nde*I and *Xho*I restriction sites. The PCR product was inserted into the pET-30a bacterial expression vector. The recombinant plasmid was inserted into *E. coli* strain BL21 (DE3) cells (TransGen Biotech, Beijing, China). Gene expression was induced by adding 1 mM isopropyl β-D-thiogalactopyranoside (IPTG) to the bacterial culture, which was incubated for 5 h until the OD_{600} reached 0.6. The expressed proteins were extracted by a centrifugation at 13,800 *g* for 5 min and then separated by SDS-PAGE. Additionally, the nucleotide sequence encoding the N-Dy10-m619SN deduced amino acid sequence was amplified using the F4/R4 primer pair (Table S4) and then inserted into pET-30a for the subsequent expression in *E. coli* as described above.

Transient expression in immature endosperm

Transient expression assays were conducted using wheat endosperm at 14 dpa. The full-length *Dy10* and *Dy10-m619SN* CDSs were amplified with the F7/R7 primer pair (Table S4) and then inserted into the

pCAMBIA1302 vector. The expression of the constructs comprising *Dy10* and *Dy10-m619SN* fused to the gene encoding the green fluorescent protein (GFP) was under the control of the CaMV 35S promoter. The resulting recombinant plasmids (p1302-Dy10-GFP and p1302-Dy10-m619SN-GFP) were inserted into separate immature endosperm samples via particle bombardment. The transformed endosperm samples were incubated at 25°C for 48 h (Vicente-Carbajosa et al. 1998). The empty vector was used as a control. The expressed proteins were detected in a western blot using a rabbit anti-GFP polyclonal antibody (1:2,000; Abcam, Cambridge, UK) and an HRP-conjugated anti-rabbit secondary antibody (1:5,000; Sigma-Aldrich).

Measurement of protein body sizes

Wheat caryopses were collected at 21 dpa and quickly cut into 2-mm slices starting from the center. The slices were fixed, rinsed, and dehydrated, after which they were embedded in resin at room temperature and polymerized at 55°C. Sections (1 μm thick) were prepared and stained for 45 s with 1% naphthol blue black dye prepared in 7% (v/v) acetic acid. Images were captured using a Zeiss Axiophot light microscope (Zeiss, Oberkochen, Germany). Protein body sizes were analyzed using ArcMap™ and ArcGIS™ software packages (ESRI, Redlands, CA, USA) as previously described (Savill et al. 2018). Analyses were completed with three biological replicates.

Scanning electron microscopy

To compare the microstructures of the WT and mutant samples, mature seeds and freeze-dried dough were prepared, with three biological replicates per treatment. All samples were carefully deposited on a silicon wafer. After spraying samples with gold particles, they were analyzed using the SEM-3500 system (Hitachi High-Technologies Corp., Tokyo, Japan). Images of the gluten networks were quantitatively analyzed using the AngioTool64 software (version 0.6a) (National Cancer Institute, National Institute of Health, Maryland, USA) (Bernklau et al. 2016).

Measurement of processing quality parameters

The mature grains for each line in field trials were harvested and milled, after which the flour was prepared for analyses of typical processing trait parameters.

Seed moisture was adjusted to 16.5% prior to milling with the CD1 Laboratory Mill (CHOPIN Technologies, Villeneuve-la-Garenne Cedex, France). The grain protein content, Zeleny sedimentation value, wet gluten content, and gluten index were determined based on the standard method in GB/T 17320 – 2013. Specifically, the Kjelec 8400 automatic azotometer (FOSS, Bremen, Denmark), a Zeleny analysis system (CAU-B, Beijing, China), and a Glutomatic 2200 system (Perten, Huddinge, Sweden) were used. Rheological properties were determined with a standard farinograph (Brabender GmbH & Co, KG, Germany), following the AACC Approved Method 54 – 21 (AACC International 2010).

The glutenin macropolymer (GMP) content was analyzed as previously described with some modifications (Jie et al. 2006). Briefly, flour samples (0.1 g) were mixed with 0.8 mL 50% (v/v) propan-1-ol

for 30 min and then centrifuged for 3 min at 6,500 *g*. The supernatant was removed and the pellet was resuspended in 0.8 mL 50% (v/v) propan-1-ol containing 2% (w/v) DTT for 1 h at 60°C. The suspension was centrifuged for 10 min at 6,500 *g*. Each extraction step was repeated three times. The supernatant was mixed with isopyknic turbidimetry reagents [1.2% (w/v) 5-sulfosalicylic acid and 0.8% (w/v) sodium sulfate] for 20 min at 25°C. The absorbance was measured at 540 nm with a Microplate Reader (Thermo Scientific). The GMP content was calculated using Albumin Bovine V (Solarbio, Beijing, China) as the standard.

Glutenins and gliadins were extracted and analyzed as previously described (Ting et al. 2018). Additionally, a baking test was performed using a published procedure (Xu et al. 2018). The baking procedure (standard rapid-mix-test) was completed using 36 g flour at 14% moisture content, with two replicates per sample. The loaf volume was determined with the BVM6630 volume meter (Perten, Stockholm, Sweden) following the manufacturer's instructions. Biscuits were prepared and evaluated according to the AACC Approved Method 10–52 (AACC International 2010).

Statistical analysis

The Chi-squared (χ^2) test was used for the segregation analysis, whereas the *t*-test was used to determine the significance of any differences. Data analyses were completed with the Data Procession System software (version 12.01) (Zhejiang University, Hangzhou, China) (Tang and Zhang 2013).

Results

Identification of the *Dy10-m619SN* allele

A mutant with six HMW-GSs, which were detected as distinct bands on an SDS-PAGE gel, was isolated after treating 'Shumai 482' seeds with 0.8% EMS. No significant differences in agronomic characteristics were detected between the WT and mutant after backcrossing (Fig. 1a–d and Table S1). The SDS-PAGE analysis indicated that in addition to the five normally expressed HMW-GSs, the mutant has an extra protein band in the HMW-GS zone that is smaller than the Dy10 subunit of the WT wheat (Fig. 1e). The extra protein band was confirmed as a HMW-GS in an immunoblot involving rabbit anti-HMW-GS glutenin polyclonal antibodies, which can cross-react with both x- and y-type subunits (Fig. 1f).

Considering that the Ay subunit is not expressed in 'Shumai 482', but is normally expressed in some wheat materials (Jiang et al. 2009; Roy et al. 2018; Wang et al. 2018), we cloned the Ay gene sequence (same as GenBank No.: MF429893) and confirmed that it is silenced in both 'Shumai 482' and the mutant. The Ay coding region includes four premature stop codons. Additionally, a PCR product corresponding to the expected size of the Ay coding region was not amplified when cDNA derived from young seeds was used as the template. Thus, the extra protein detected in the mutant is not the Ay subunit.

To identify the genomic loci associated with the extra protein, the mutant line was crossed with 'Chinese Spring'. An SDS-PAGE analysis indicated that the extra protein band was associated with Dx5 + Dy10 in the F_2 population. Moreover, the distribution of the genotypes [*Dx5* + *Dy10* (with the extra protein): heterozygous: *Dx2* + *Dy12*] in 257 seeds conformed to a Mendelian ratio of 1:2:1 (Table 1). The x- and y-type HMW-GS genes at the *Glu-D1* locus are tightly linked (Payne 1987). These findings suggest that the gene encoding the extra protein is a new *Dx5* or *Dy10* allele.

Table 1
Segregation analysis (based on SDS-PAGE) of the HMW-GS phenotypes of seeds in the F_2 generation derived from the mutant × 'Chinese Spring' cross

Genotypes	No. of seeds	Expected ratio	*χ2*	*P*
Dx2 + *Dy12*	61	1:2:1	0.533	0.766
Heterozygote	127			
Dx5 + *Dy10* (with the extra protein)	69			

To identify the extra protein, the corresponding band was manually cut from the SDS-PAGE gel. The subsequent analysis by mass spectrometry revealed that two peptides (QVVDQQLAGRLPWSTGLQMR and SVAVSQVAR) from the extra protein subunit are identical to Dy10, but differ from the other HMW-GSs (Fig. S2b and S2c). This implies that the extra protein is derived from the Dy10 subunit.

The differences in the electrophoretic mobility among the HMW-GSs in the SDS-PAGE gel are mainly due to variations in the number of repeating units comprising the central repetitive domain (Shewry et al. 1995) as well as amino acid substitutions (Li et al. 2014; Wang et al. 2016). A single amino acid substitution in the Dy10 subunit increased the stability of the secondary structure, protecting it from the denaturant SDS and increasing the mobility of the protein in the SDS-PAGE gel. However, the protective effect of the amino acid change may be eliminated by the addition of urea, which is a stronger denaturant than SDS, capable of thoroughly breaking down the secondary structure of proteins (Lafiandra et al. 1999; Wang et al. 2016). Thus, the SDS-PAGE analysis was repeated with a gel containing urea. In contrast to our results from an earlier study (Wang et al. 2016), the extra protein exhibited greater mobility than Dy10 in the presence of urea (Fig. 1g). Furthermore, similar to *Dy10* (GenBank No.: X12929) in the WT wheat, the cloned open reading frame of *Dy10* (GenBank No.: MW001617) in the mutant comprises 1,947 bp and encodes 648 residues (Fig. S2a), with no deletion of repeating units detected at the DNA and RNA levels (Fig. 1h).

Despite the sequence similarities, a missense mutation (G to A) was identified (Fig. S2a), resulting in a serine (Ser)-to-asparagine (Asn) substitution at the 619th residue within the C-terminal domain (Fig. S1e). To efficiently detect the point mutation and develop suitable markers for molecular breeding, specific KASP markers were designed (Fig. S1c). This new *Dy10* allele was designated as *Dy10-m619SN*, and the

observed protein bands on the SDS-PAGE gel corresponded to the full-length Dy10-m619SN (Full-Dy10-m619SN) and the extra protein N-Dy10-m619SN. To assess the possibility of alternative splicing during transcription, cDNA samples derived from the immature seeds [i.e., 25 dpa] of the mutant were used as the templates for amplifying the CDS and the 3' UTR. The results revealed a lack of spliced sequences (Fig. 1h and Fig. S2d), which is consistent with a partial post-translational cleavage of *Dy10-m619SN*.

Partial post-translational cleavage of *Dy10-m619SN*

To determine whether N-Dy10-m619SN is produced because of a post-translational cleavage, Dy10 from the WT wheat as well as Full-Dy10-m619SN and N-Dy10-m619SN from the mutant underwent C-terminal sequencing. Notably, Dy10, Full-Dy10-m619SN, and N-Dy10-m619SN respectively included HVSAEQQAASPM, HVSAEQQAANPM, and HVSAEQQAAN sequences (Fig. 2a). These results imply that N-Dy10-m619SN is the product of a partial post-translational cleavage of Full-Dy10-m619SN after the 619th residue (Asn). The authenticity of the N-Dy10-m619SN subunit was confirmed by bacterial expression (Fig. 2b).

To further analyze this cleavage in developing seeds, the proteins in wheat seeds collected at specific time-points after anthesis were analyzed by SDS-PAGE. The protein bands corresponding to Full-Dy10-m619SN and N-Dy10-m619SN were simultaneously observed as early as 14 dpa (Fig. 2c).

To confirm that N-Dy10-m619SN is the result of a post-translational cleavage of Full-Dy10-m619SN and to detect the downstream peptide (C-Dy10-m619SN) after the cleavage, a fusion construct comprising the *Dy10-m619SN* CDS and the GFP-encoding gene was transiently expressed in immature wheat endosperm. The two proteins detected by the anti-GFP antibody [Fig. 2e (lane 3)] were revealed to be Full-Dy10-m619SN (higher molecular mass) and C-Dy10-m619SN (lower molecular mass). However, N-Dy10-m619SN was not detected by the antibody because it was not tagged with GFP. In contrast, only one protein band with the same molecular mass as Full-Dy10-m619SN was detected when the WT Dy10-GFP protein was expressed [Fig. 2e (lane 4)]. These observations indicate that Full-Dy10-m619SN is partially cleaved to produce N-Dy10-m619SN and C-Dy10-m619SN *in vivo*.

Effects of *Dy10-m619SN* on HMW-GS accumulation

To evaluate the extent of the cleavage in mature seeds, we determined the relative contents of Full-Dy10-m619SN and N-Dy10-m619SN in the mutant. The calculated proportions of Full-Dy10-m619SN and N-Dy10-m619SN were 47.4% and 52.6%, respectively (Fig. 2d), and the abundance of the latter was significantly greater than that of the former ($P < 0.01$).

Effects of *Dy10-m619SN* on gluten microstructure

To investigate the overall features of storage protein accumulation, the protein body content in the semi-thin section of the endosperm was analyzed. In the mutant section, small protein bodies (0.2–0.5 μm^2) represented 38–45% of the total content in each zone, which was substantially higher than the proportion

in the WT sections (23–30%) (Fig. 3a and 3b). The proportions of the other protein bodies (1.5–228.8 μm^2) were significantly lower in the mutant sections than in the WT sections. Next, the microstructures of mature WT and mutant seeds were compared with a scanning electron microscope. We detected more protein matrix tightly adhered to starch granules in the WT samples than in the mutant samples (Fig. S3a). Additionally, the GMP content was significantly lower in the mutant than in the WT ($P < 0.05$) (Table 2). These data clearly indicate that the partial post-translational cleavage decreases glutenin polymer size.

Table 2
Comparison of the major parameters related to quality traits, rheological properties, and baking quality between the WT and mutant

Parameter	2017–2018 BC2F4, Field		BC2F4, Greenhouse		2019–2020 BC3F4, Field	
	WT	mutant	WT	mutant	WT	mutant
Quality trait						
Grain protein content (%)	13.05 ± 0.41	12.86 ± 0.14	12.52 ± 0.14	12.49 ± 0.02	13.55 ± 0.42	13.42 ± 0.67
Zeleny sedimentation value (mL)	23.66 ± 1.58	18.94 ± 0.77**	23.48 ± 0.41	17.88 ± 0.30**	19.31 ± 1.68	16.15 ± 2.53*
Wet gluten content (%)	21.77 ± 1.27	23.51 ± 1.13**	16.48 ± 0.56	18.53 ± 0.39**	23.85 ± 1.55	26.70 ± 0.93**
Gluten index (%)	96.84 ± 1.05	85.93 ± 4.56**	98.75 ± 0.44	95.13 ± 1.95*	74.84 ± 9.63	48.86 ± 2.98**
GMP (%)	1.89 ± 0.18	1.42 ± 0.29**	2.95 ± 0.03	2.39 ± 0.33**	1.95 ± 0.20	1.55 ± 0.20**
Rheological property						
Dough development time (min)	1.47 ± 0.17	1.32 ± 0.10**	0.87 ± 0.06	0.85 ± 0.10	1.39 ± 0.08	1.26 ± 0.10*
Dough stability time (min)	6.24 ± 1.76	4.04 ± 0.56*	1.30 ± 0.10	0.93 ± 0.15*	4.59 ± 1.26	2.91 ± 1.15*
Softness of 10 min (FE)	65.09 ± 17.64	84.43 ± 10.40**	122.67 ± 5.77	135.00 ± 13.00	67.58 ± 10.58	93.17 ± 18.12*
Baking quality						
Loaf volume (mL)	225.75 ± 5.57	217.88 ± 5.58**	—	—	188.29 ± 8.71	170.86 ± 9.06**
Biscuit Diameter (mm)	101.23 ± 1.55	104.76 ± 1.86**	—	—	104.58 ± 1.99	108.17 ± 1.29**
Biscuit Height (mm)	8.48 ± 0.63	8.07 ± 0.36**	—	—	8.74 ± 0.63	7.78 ± 0.13**

Data are presented as the mean ± standard deviation.

* and ** represent significant differences at $P < 0.05$ and $P < 0.01$, respectively.

To assess the possible interference by the glutenin and gliadin contents and compositions, we analyzed the grain protein, gliadin, and glutenin contents. There was no significant difference in the grain protein contents (Table 2) and the gliadin contents (Table S2) between the WT and mutant samples. Interestingly, the glutenin content was slightly but significantly lower in the mutant samples than in the WT samples (*P*

< 0.01), possibly because of differences in peptide solubility resulting from the post-translational cleavage.

Effects of *Dy10-m619SN* on wheat processing quality

To evaluate the effects of *Dy10-m619SN* on wheat processing quality parameters, the wet gluten content, gluten index, Zeleny sedimentation value, and dough rheological properties were compared between the WT and mutant. The data revealed that the wet gluten content of the mutant was significantly higher than that of the WT. In contrast, the Zeleny sedimentation value and gluten index were lower in the mutant than in the WT. Moreover, the dough development and stability times (i.e., rheological properties) were significantly shorter for the mutant than for the WT (Table 2). These data indicate that the post-translational cleavage decreases dough strength.

To confirm the effects of the post-translational cleavage on dough strength, we examined the microstructure of the gluten network. The freeze-dried gluten from the WT and mutant samples was analyzed with a scanning electron microscope. The images of the WT gluten revealed diverse aperture sizes, which was in contrast to the uniform and compact apertures detected in the images of the mutant gluten (Fig. 3c). A quantitative analysis of the images revealed more protein junctions and a higher junction density in the mutant than in the WT. Furthermore, gluten lacunarity [i.e., the number and size of network gaps, reflecting structural irregularities], which was used as an indicator of dough strength, was significantly lower in the mutant than in the WT (Table S3). These findings suggest the gluten profile is weaker in the mutant than in the WT.

We also analyzed the bread-making quality based on the loaf volume. Specifically, the loaf volume was significantly lower for the mutant wheat than for the WT wheat ($P < 0.05$) (Fig. 4a and Table 2). However, the biscuit quality (i.e., diameter and thickness) was higher for the mutant wheat than for the WT wheat (Fig. 4b and Table 2).

Discussion

The HMW-GSs are the main determinants of end-use quality because of their distinct molecular structures, especially their interchain disulfide bonds (Shewry et al. 1992, 2003a). The HMW-GS polymer backbone is established by end-to-end or head-to-tail linkages due to interchain disulfide bonds (Graveland et al. 1985; Wieser 2007). The basic molecular unit of glutenin polymers might consist of two y-type HMW-GSs, four x-type HMW-GSs, and many LMW-GSs covalently linked by interchain disulfide bonds (Wieser 2007). Consistent with the reported data, we proposed a model for glutenin polymers that explains the effect of *Dy10-m619SN* on wheat processing quality (Fig. 5). The Cys residue in the C-terminal domain of Dy10 (identical to the Cys in C-Dy10-m619SN) is essential for the formation of the interchain disulfide bonds that contribute to the elongation of glutenin polymers. We applied a series of approaches to demonstrate the partial post-translational cleavage at the C-terminal domain of Full-Dy10-m619SN. Additionally, Full-Dy10-m619SN (seven Cys residues) can be efficiently processed (52.6%) into N-Dy10-m619SN (six Cys) and C-Dy10-m619SN (one Cys). The change in the number of Cys residues in

these two peptides leads to the production of competitive chain terminators (Fig. 5b and 5c) and decreases the glutenin polymer size and dough strength, ultimately resulting in increased cookie-making quality (Table 2).

Silencing HMW-GS genes represents one strategy for breeding soft wheat. However, there are reportedly positive and negative effects associated with this approach. For example, the deletion of a single HMW-GS gene in the Ningmai 9 soft wheat variety resulted in increased sugar snap cookie-making quality (Zhang et al. 2016). In contrast, other studies revealed that the absence of HMW-GSs Dy12 (Chen et al. 2021), Bx7 and By9 (Chen et al. 2019), leads to decreased cake and biscuit quality, possibly because of the associated decrease in glutenin content and increased gliadin content. The polymeric glutenins are mostly responsible for dough elasticity, whereas the monomeric gliadins influence extensibility-related characteristics (Hoseney 1986). Thus, the glutenin-to-gliadin ratio can directly affect the balance between dough strength and extensibility, making it critical for the quality of end products (Barak et al. 2013; Wrigley et al. 2006). In this study, the weakening of gluten due to *Dy10-m619SN* was reflected by the gluten microstructure and certain processing quality parameters. Additionally, *Dy10-m619SN* did not affect the glutenin-to-gliadin ratio, but it improved the cookie-making quality of wheat. Therefore, the post-translational cleavage of HMW-GSs is an important consideration for the breeding of soft wheat.

Several studies proved that Full-Dy10-m619SN can be efficiently cleaved after the Asn residue (Gruis et al. 2004; Hara-Nishimura et al. 1995, 2004; Kumamaru et al. 2010; Wang et al. 2009). Two conserved Asn residues unique to the C-terminal domain of the By subunits result in two minor proteoforms detectable on two-dimensional electrophoresis gels (Nunes-Miranda et al. 2017). The HMW-GS CDSs encoding the C-terminal domain are highly conserved, and usually do not include a codon for Asn (Fig. S4). Therefore, on the basis of the results of the current study, we hypothesize that a modest increase in the number of Asn residues in the HMW-GS C-terminal domain via site-specific mutagenesis can improve the cookie-making quality of wheat.

In conclusion, a new *Dy10* allele, *Dy10-m619SN*, was identified by screening an EMS-induced mutant population derived from the common wheat cultivar ‘Shumai 482’. A subsequent analysis revealed that *Dy10-m619SN* expression results in three peptides in the wheat endosperm because of a post-translational cleavage. Moreover, the effects of *Dy10-m619SN* on wheat processing quality as well as the underlying mechanism were clarified. This study provides researchers and breeders with new genetic information relevant for enhancing wheat quality through breeding.

Declarations

Supplementary Information The online version contains supplementary material available at

Author’ contributions

Q and Y. Z designed the experiments. Y. W, Q. C, and P. Q wrote the manuscript. P. Q and Q. C prepared the plant materials. Y. W, Q. C, Y. L, Z. G, C. L, Y. W, M. H, J. Z, W. W, M. W, K. Z, Y. J, Y. Z, Q. X, L. K, Z. P, M. D, Q.

J, X. L, J. W, G. C, J. M, Y. Z, Y. W, and P. Q conducted the experiments, analyzed the data, and provided key advice. All authors discussed the results and helped revise the manuscript.

Acknowledgments

We thank Prof. Peter Shewry at Rothamsted Research and Dr. Yufeng Hu at Sichuan Agricultural University for technical assistance. We acknowledge Liwen Bianji, Edanz Editing China (www.liwenbianji.cn/ac) for editing the English text of a draft of this manuscript.

Funding

This study was supported by the National Natural Science Foundation of China (grant numbers 31971939, 31671677, and 32072054), the Science and Technology Department of Sichuan Province (2019YFH0066, 20GJHZ0048, and 2018NZDZX002), and the Designing Future Wheat strategic program (BB/P016855/1) of the UK. Yan Wang acknowledges funding by the China Scholarship Council.

Ethics approval and consent to participate Not applicable

Consent for publication Not applicable

Consent for publication Not applicable.

References

AACC International (2010) Approved Methods of Analysis, 11th edn, St. Paul, MN, 2010. http://methods.aaccnet.org/

Anderson OD, Greene FC (1989) The characterization and comparative analysis of high-molecular-weight glutenin genes from genomes A and B of a hexaploid bread wheat. Theor Appl Genet 77:689–700..https://doi.org/10.1007/BF00261246

Barak S, Mudgil D, Khatkar BS (2013) Relationship of gliadin and glutenin proteins with dough rheology, flour pasting and bread making performance of wheat varieties. LWT - Food Sci Technol 51:211–217. https://doi.org/10.1016/j.lwt.2012.09.011

Barak S, Mudgil D, Khatkar BS (2015) Biochemical and functional properties of wheat gliadins: a review. Crit Rev Food Sci Nutr 55:357–368. https://doi.org/10.1080/10408398.2012.654863

Barro F, Barceló P, Lazzeri PA, et al (2003) Functional properties of flours from field grown transgenic wheat lines expressing the HMW glutenin subunit 1Ax1 and 1Dx5 genes. Mol Breed 12:223–229. https://doi.org/10.1023/A:1026367214120

Bernklau I, Lucas L, Jekle M, Becker T (2016) Protein network analysis — A new approach for quantifying wheat dough microstructure. Food Res Int 89:812–819. https://doi.org/10.1016/j.foodres.2016.10.012

Blechl A, Lin J, Nguyen S, et al (2007) Transgenic wheats with elevated levels of Dx5 and/or Dy10 high-molecular-weight glutenin subunits yield doughs with increased mixing strength and tolerance. J Cereal Sci 45:172–183. https://doi.org/10.1016/j.jcs.2006.07.009

Chen H, Li S, Liu Y, et al (2021) Effects of 1Dy12 subunit silencing on seed storage protein accumulation and flour-processing quality in a common wheat somatic variation line. Food Chem 335:127663. https://doi.org/10.1016/j.foodchem.2020.127663

Chen Q, Zhang W, Gao Y, et al (2019) High molecular weight glutenin subunits 1Bx7 and 1By9 encoded by *Glu-B1* locus affect wheat dough properties and sponge cake quality. J Agric Food Chem 67:11796–11804. https://doi.org/10.1021/acs.jafc.9b05030

Hoseney RC (1986) Principles of cereal science and technology, 2nd ed, St. Paul, MN. https://doi.org/10.1002/star.19870390416

Denery-Papini S, Popineau Y, Quillien L, Van Regenmortel M (1996) Specificity of anti sera raised against synthetic peptide fragments of high Mr glutenin subunits. J Cereal Sci 23: 133–144.

Doyle, JJ, Doyle JL (1987) A rapid DNA isolation procedure for small quantities of fresh leaf tissue. Phytochem Bull 19: 11–15.

Graveland A, Bosveld P, Lichtendonk WJ, et al (1985) A model for the molecular structure of the glutenins from wheat flour. J Cereal Sci 3:1–16. https://doi.org/10.1016/S0733-5210(85)80029-1.

Gruis D, Schulze J, Jung R (2004) Storage protein accumulation in the absence of the vacuolar processing enzyme family of cysteine proteases. Plant Cell 16:270–290. https://doi.org/10.1105/tpc.016378

Halford NG, Field JM, Blair H, et al (1992) Analysis of HMW glutenin subunits encoded by chromosome 1A of bread wheat (*Triticum aestivum* L.) indicates quantitative effects on grain quality. Theor Appl Genet 83:373–378. https://doi.org/10.1007/BF00224285

Hara-Nishimura I, Inoue K, Nishimura M (1991) A unique vacuolar processing enzyme responsible for conversion of several proprotein precursors into the mature forms. FEBS Lett 294:89–93. https://doi.org/10.1016/0014-5793(91)81349-D

Hara-Nishimura I, Shimada T, Hiraiwa N, Nishimura M (1995) Vacuolar processing enzyme responsible for maturation of seed proteins. J Plant Physiol 145:632–640. https://doi.org/10.1016/S0176-1617(11)81275-7

Jiang QT, Wei YM, Wang F, et al (2009) Characterization and comparative analysis of HMW glutenin 1Ay alleles with differential expressions. BMC Plant Biol 9:6. https://doi.org/10.1186/1471-2229-9-16

Jie WS, Hui KM, Shan YM, et al (2006) Comparison of two sorts of turbidimetry reagents in measurement of wheat glutenin macropolymer content. J Triticeae Crop 20:56–59.

Kumamaru T, Uemura Y, Inoue Y, et al (2010) Vacuolar processing enzyme plays an essential role in the crystalline structure of glutelin in rice seed. Plant Cell Physiol 51:38–46. https://doi.org/10.1093/pcp/pcp165

Lafiandra D, Turchetta T, D'Ovidio R, et al (1999) Conformational polymorphism of high Mr glutenin subunits detected by transverse urea gradient gel electrophoresis. J Cereal Sci 30:97–104. https://doi.org/10.1006/jcrs.1999.0260

Laudencia-Chingcuanco D (2012) Isolation and characterization of EMS-induced Dy10 and Ax1 high molecular weight glutenin subunit deficient mutant lines of elite hexaploid wheat (*Triticum aestivum* L.) cv. Summit. J Cereal Sci 56:296–299. https://doi.org/10.1016/j.jcs.2012.06.009

Lawrence GJ, MacRitchie F, Wrigley CW (1988) Dough and baking quality of wheat lines deficient in glutenin subunits controlled by the *Glu-A1*, *Glu-B1* and *Glu-D1* loci. J Cereal Sci 7:109–112. https://doi.org/10.1016/S0733-5210(88)80012-2

León E, Marín S, Giménez MJ, et al (2009) Mixing properties and dough functionality of transgenic lines of a commercial wheat cultivar expressing the 1Ax1, 1Dx5 and 1Dy10 HMW glutenin subunit genes. J Cereal Sci 49:148–156. https://doi.org/10.1016/j.jcs.2008.08.002

Li Y, An X, Yang R, et al (2014) Dissecting and enhancing the contributions of high-molecular-weight glutenin subunits to dough functionality and bread quality. Mol Plant 8:332–334. https://doi.org/10.1093/mp/ssu118

Müntz K (1998) Deposition of storage proteins. Plant Mol Biol 38:77–99. https://doi.org/10.1007/978-94-011-5298-3_4

Nunes-Miranda JD, Bancel E, Viala D, et al (2017) Wheat glutenin: the "tail" of the 1By protein subunits. J Proteomics 169:136–142. https://doi.org/10.1016/j.jprot.2017.05.019

Payne PI, Holt LM, Law CN (1981) Structural and genetical studies on the high-molecular-weight subunits of wheat glutenin - Part 1: Allelic variation in subunits amongst varieties of wheat (*Triticum aestivum*). Theor Appl Genet 60:229–236. https://doi.org/10.1007/BF02342544

Payne PI, Holt LM, Law CN (1982) Structural and genetical studies on the high-molecular-weight subunits of wheat glutenin - Part 3. Telocentric mapping of the subunit genes on the long arms of the homoeologous Group 1 chromosomes. Theor Appl Genet 63:129–138. https://doi.org/10.1007/BF02342544

Payne PI (1987) Genetics of wheat storage proteins and the effect of allelic variation on breadmaking quality. Annu Rev Plant Biol 38:141–153 https://doi.org/10.1146/annurev.pp.38.060187.001041

Qi PF, Wei YM, Yue YW, et al (2006) Biochemical and molecular characterization of gliadins. Mol Biol 40:713–723. https://doi.org/10.1134/S0026893306050050

Qi PF, Wei YM, Chen Q, et al (2011) Identification of novel α-gliadin genes. Genome 54:244–252. https://doi.org/10.1139/G10-114

Roy N, Islam S, Ma J, et al (2018) Expressed Ay HMW glutenin subunit in Australian wheat cultivars indicates a positive effect on wheat quality. J Cereal Sci 79:494–500. https://doi.org/10.1016/j.jcs.2017.12.009

Savill GP, Michalski A, Powers SJ, et al (2018) Temperature and nitrogen supply interact to determine protein distribution gradients in the wheat grain endosperm. J Exp Bot 69:3117–3126. https://doi.org/10.1093/jxb/ery127.

Shewry PR, Halford NG, Tatham AS (1992) The high molecular weight subunits of wheat glutenin. J Cereal Sci 15:105–120

Shewry PR, Tatham AS, Halford NG (1999) The prolamins of the Triticeae. In Seed proteins, Shewry PR, Casey R, Eds, Kluwer Academic Publishers, Dordrecht, pp 35-78. https://doi.org/10.1007/978-94-011-4431-5_3

Shewry PR, Halford NG (2002) Cereal seed storage proteins: Structures, properties and role in grain utilization. J Exp Bot 53:947–958. https://doi.org/10.1093/jexbot/53.370.947

Shewry PR, Halford NG, Tatham AS, et al (2003a) The high molecular weight subunits of wheat glutenin and their role in determining wheat processing properties. Adv Food Nutr Res 45:219–302. https://doi.org/10.1016/s1043-4526(03)45006-7

Shewry PR, Halford NG, Lafiandra D (2003b) Genetics of wheat gluten proteins. Adv Genet 49:111–184.

Tang QY, Zhang CX (2013) Data Processing System (DPS) software with experimental design, statistical analysis and data mining developed for use in entomological research. Insect Sci 20:254–260. https://doi.org/10.1111/j.1744-7917.2012.01519.x

Vicente-Carbajosa J, Oñate L, Lara P, et al (1998) Barley BLZ: A bZIP transcriptional activator that interacts with endosperm-specific gene promoters. Plant J 13:629–640. https://doi.org/10.1111/j.1365-313X.1998.00068.x

Wan Y, Gritsch CS, Hawkesford MJ, Shewry PR (2014) Effects of nitrogen nutrition on the synthesis and deposition of the ω-gliadins of wheat. Ann Bot 113:607–615. https://doi.org/10.1093/aob/mct291

Wang Y, Zhu S, Liu S, et al (2009) The vacuolar processing enzyme OsVPE1 is required for efficient glutelin processing in rice. Plant J 58:606–617. https://doi.org/10.1111/j.1365-313X.2009.03801.x

Wang Y, Zheng QY, Guo ZR, et al (2016) A missense mutation affects the mobility of high molecular weight glutenin Dy10 subunit in SDS-PAGE. Agri Gene 2:1–4. https://doi.org/10.1016/j.aggene.2016.09.001

Wang Z, Huang L, Wu B, et al (2018) Characterization of an integrated active *glu-1ay* allele in common wheat from wild emmer and its potential role in flour improvement. Int J Mol Sci 19:923. https://doi.org/10.3390/ijms19040923

Wieser H (2007) Chemistry of gluten proteins. Food Microbiol 24:115–119. https://doi.org/10.1016/j.fm.2006.07.004

Wrigley C, Bekes F, Bushuk W (2006) Gliadin and glutenin. In: The unique Balance of wheat quality, 1st ed, AACC International, MN, pp 3–32. https://doi.org/DOI: 10.1094/9781891127519.002.

Xu BJ, Chen Q, Zheng T, et al (2018) An overexpressed *Q* allele leads to increased spike density and improved processing quality in common wheat (*Triticum aestivum*). G3 Genes, Genomes, Genet 8:771–778. https://doi.org/10.1534/g3.117.300562

Yan Y, Hsam SLK, Yu J, et al (2003) Allelic variation of the HMW glutenin subunits in *Aegilops tauschii* accessions detected by sodium dodecyl sulphate (SDS-PAGE), acid polyacrylamide gel (A-PAGE) and capillary electrophoresis. Euphytica 130:377–385. https://doi.org/10.1023/A:1023062316439

Zhang YZ, Wei ZZ, Liu CH, et al (2017) Linoleic acid isomerase gene *FgLAI12* affects sensitivity to salicylic acid, mycelial growth and virulence of *Fusarium graminearum*. Sci Rep 7:46129. https://doi.org/10.1038/srep46129

Zhang P, Ma H, Yao J, et al (2016) Effect of HMW-GS Deletion on Processing Quality of Soft Wheat Ningmai 9. Acta Agron Sin 42:633–640. https://doi.org/10.3724/SP.J.1006.2016.00633

Zheng T, Qi PF, Cao YL, et al (2018). Mechanisms of wheat (*Triticum aestivum*) grain storage proteins in response to nitrogen application and its impacts on processing quality. Sci Rep 8:11928. https://doi.org/10.1038/s41598-018-30451-4

Figures

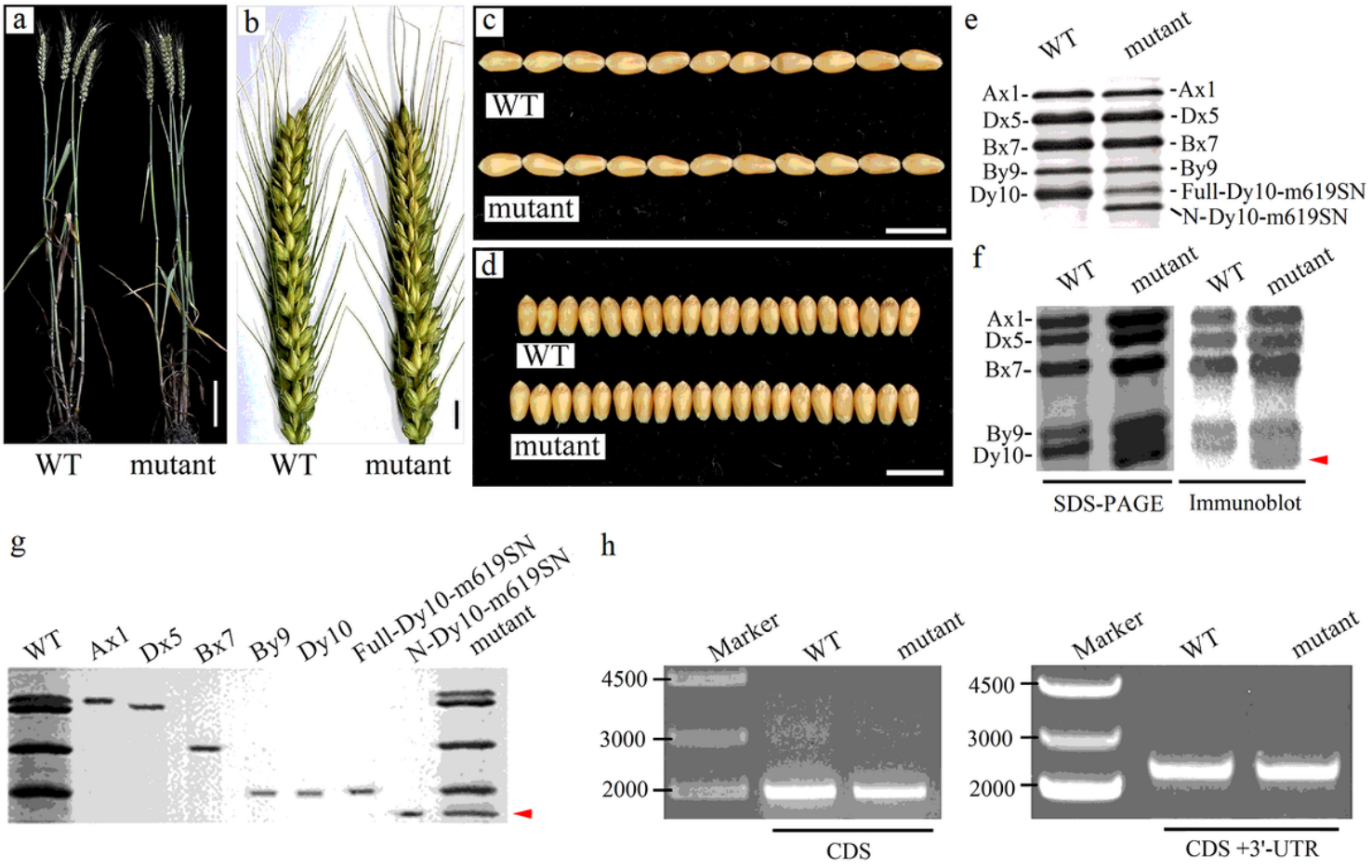

Figure 1

Identification of the Dy10-m619SN allele. (a–d) Morphological features of the WT and mutant plants. (a) Plant morphology, scale bar: 10 cm. (b) Ear trait, scale bar: 1 cm. (c) Kernel length, scale bar: 1 cm. (d) Kernel width, scale bar: 1 cm. (e–g) SDS-PAGE analysis of the HMW-GSs. (e) HMW-GS compositions in the WT and mutant. (f) Immunoblot analysis of the WT and mutant using the anti-HMW-GS antibody. (g) SDS-PAGE analysis with 4 M urea. Individual bands representing the HMW-GSs were excised from the gel and identified. (h) Separation of PCR-amplified Dy10 gene sequences in a 1.5% agarose gel. The coding sequence (CDS) from genomic DNA (left) and the CDS + 3' untranslated region (UTR) from cDNA (right) are presented. The red arrowheads in (f) and (g) indicate the extra protein band.

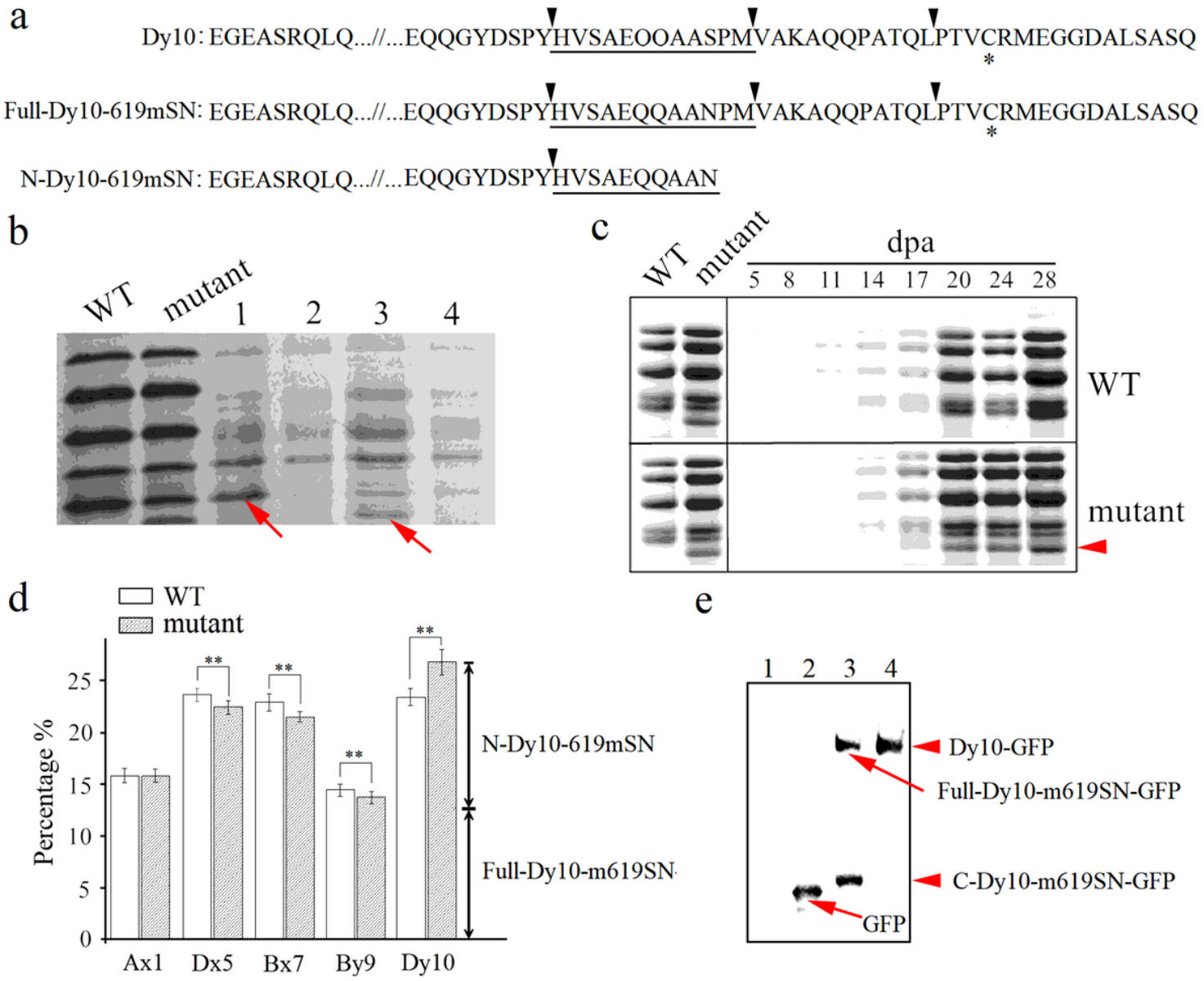

Figure 2

N-Dy10-m619SN is the result of a post-translational cleavage. (a) Analysis of the C-terminal sequences of Dy10, Full-Dy10-m619SN, and N-Dy10-m619SN. Downward-pointing arrows indicate the cleavage sites for chymotrypsin. The underlined peptides indicate post-translational cleavage. The asterisks indicate cysteine residues. (b) Verification of the coding sequence by the heterologous expression in E. coli. The proteins extracted from E. coli expressing Full-Dy10-m619SN (lanes 1 and 2) and N-Dy10-m619SN (lanes 3 and 4) with (lanes 1 and 3) and without (lanes 2 and 4) IPTG are presented. Red arrowheads indicate Full-Dy10-m619SN (lane 1) and N-Dy10-m619SN (lane 3). (c) Dynamic accumulation of HMW-GSs in the WT and mutant at different time-points [days post-anthesis (dpa)]. The red arrow indicates the extra protein band (N-Dy10-m619SN) in the mutant. (d) Comparison of the HMW-GS contents in the WT and mutant. Asterisks indicate significance at $P < 0.01$. (e) Transient expression of Dy10-m619SN in wheat endosperm; lane 1, negative control; lane 2, GFP; lane 3, Dy10-m619SN-GFP; lane 4, Dy10-GFP.

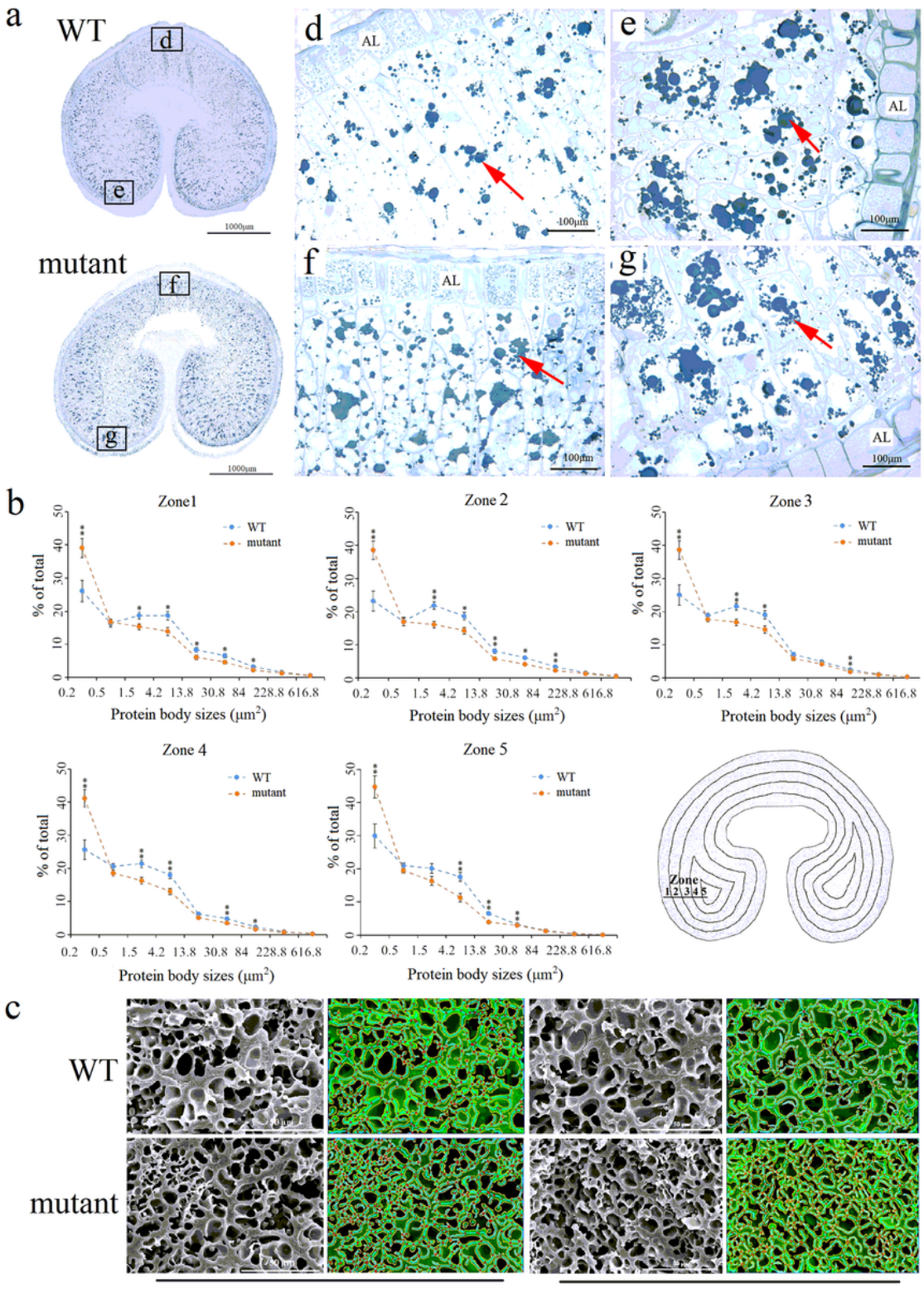

Figure 3

Effects of Dy10-m619SN allele on protein body size and the protein network. (a) Microstructures of the developing wheat endosperm of the WT (d and e) and mutant (f and g) samples at 21 dpa. Red arrows indicate protein bodies. AL, aleurone layer. (b) Frequencies of different protein body sizes in each of the five endosperm zones at 21 dpa. * and ** indicate significance at $P < 0.05$ and $P < 0.01$, respectively. (c) Protein network analysis of freeze-dried gluten samples. Specific details are provided in Table S3.

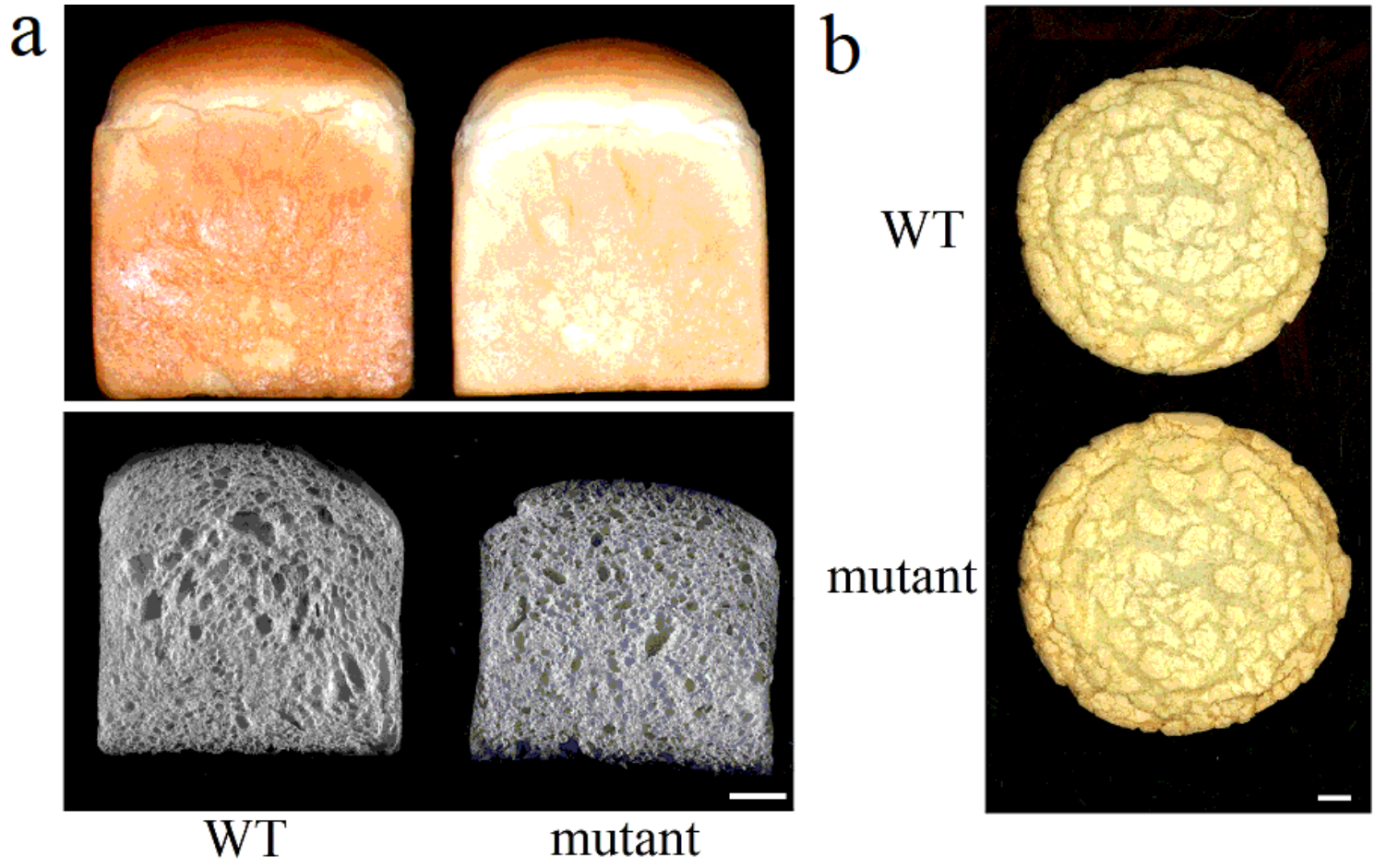

Figure 4

Effects of Dy10-m619SN allele on the end-use quality. (a) Loaf shapes and slices of bread produced from WT (left) and mutant (right) wheat. Scale bar = 1 cm. (b) Appearance of biscuits produced from WT and mutant wheat. Scale bar = 1 cm. Specific details are provided in Table 2.

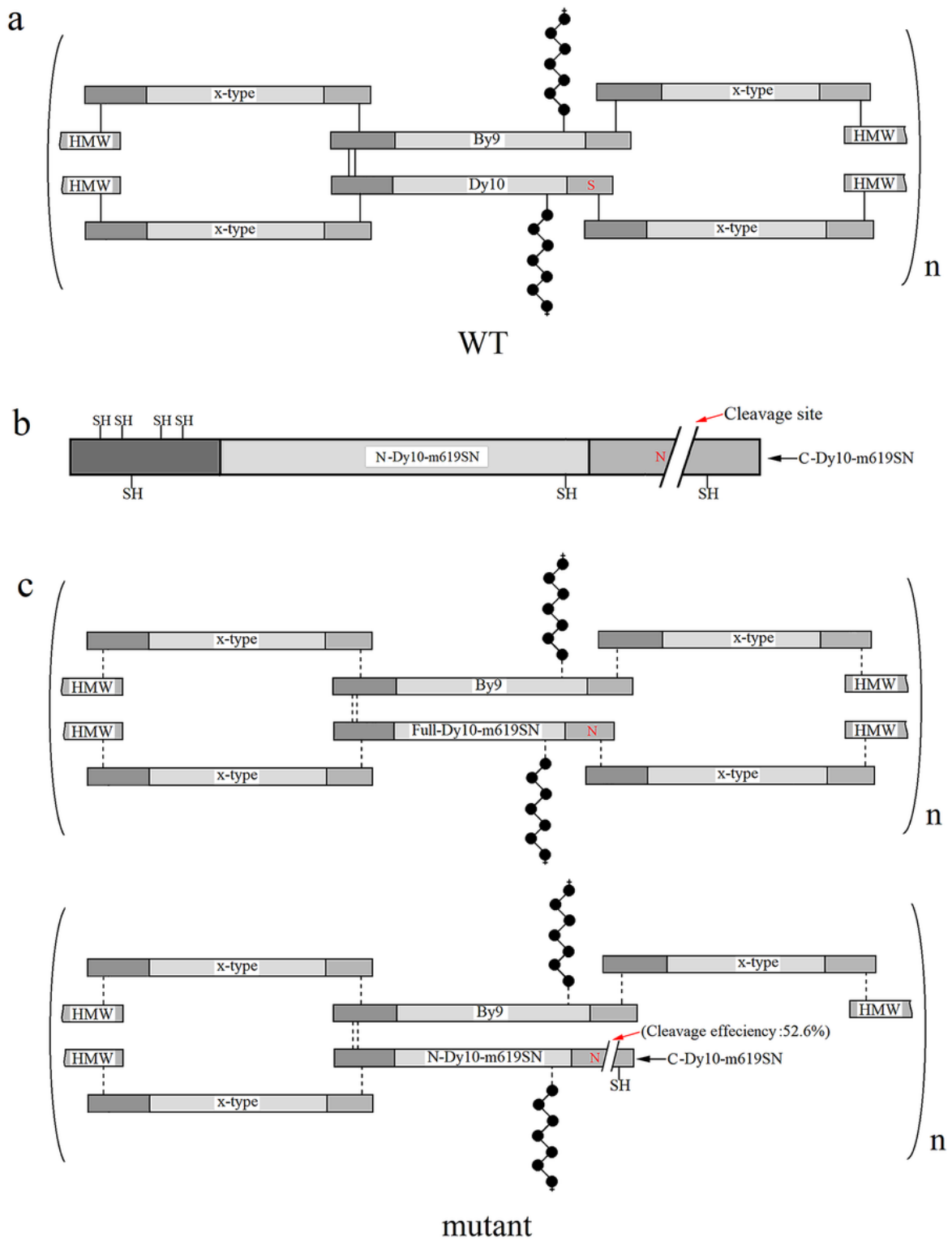

Figure 5

Proposed model for gluten polymers, in which HMW-GSs and LMW-GSs are linked by interchain disulfide structures. (a) Model of the WT gluten polymers. (b) Full-Dy10-m619SN is cleaved after the Asn site, which changes the number of cysteine residues in the peptides. '-SH' indicates the free sulfhydryl of cysteine. (c) Model of the mutant gluten polymers. Dashed lines indicate potential interaction sites

resulting from the competition involving N-Dy10-m619SN and C-Dy10-m619SN as chain terminators. ‘S’ and ‘N’ in red respectively indicate the serine (Ser) and asparagine (Asn) at the 619th residue.